ACS OMEGA

Open Access

http://pubs.acs.org/journal/acsodf

Article

Preparation and Properties of Sodium Carboxymethyl Cellulose Microspheres by Dropping Method

Ling Wang, De-Shuang You, Dan-yan Guo, Xue-Chen Zhuang, Tao Yuan,* and Dan Qiu*

Cite This: *ACS Omega* 2025, 10, 4754−4762

Read Online

ACCESS | Metrics & More | Article Recommendations

ABSTRACT: Sodium carboxymethyl cellulose (CMC) is the most extensively utilized derivative of cellulose. In this study, an innovative approach was employed to disperse a CMC aqueous solution into olive oil in the form of liquid droplets, resulting in the direct formation of CMC microspheres after drying. The effects of CMC concentration and needle aperture size on microsphere formation were systematically investigated, showing that the particle size of the microspheres decreased with an increase in CMC concentration and a decrease in needle aperture. The CMC-based microspheres exhibited a consistently uniform spheroid morphology with particle sizes ranging from 1.5 to 2.5 mm, and a three-dimensional uniform polymeric network structure. Furthermore, the drug loading efficiency of the CMC-based olive oil microspheres reached 82.18%, which was markedly superior to that of other cellulose-based microspheres for fat-soluble substances. The CMC-based vitamin C (VC) microspheres exhibited an ultimate drug loading efficiency of approximately 24%, and their maximum encapsulation efficiency was 78.57% at a VC concentration of 30%, which was significantly higher than that of starch-based VC microspheres. Additionally, the CMC-based VC microspheres realized a sustained and stable release rate in ethanol at 30 °C.

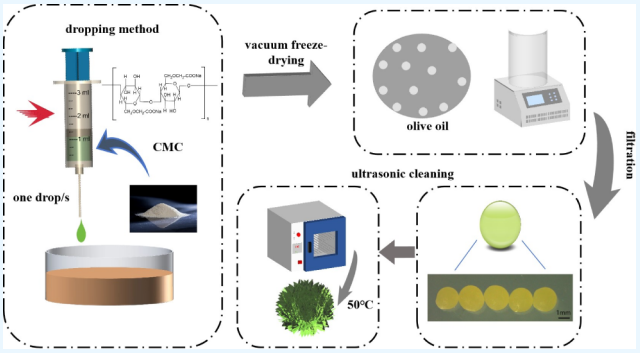

1. INTRODUCTION

Cellulose, recognized as the most abundant natural polysaccharide,[1] offers the advantages of appropriate porosity, excellent biocompatibility, ease of modification, and low production cost.[2] Microspheres derived from cellulose exhibit a porous structure, a large specific surface area, and pronounced hydrophilicity.[3] These features, coupled with their facile functional modification, facilitate their extensive range of applications.[4]

Sodium carboxymethyl cellulose (CMC) is an important cellulose derivative widely employed in numerous fields such as food, medicine, petroleum, energy storage, printing and dyeing, and daily chemicals.[5] CMC-based microspheres are novel polymer carriers. The synthesis methods of CMC-based microspheres play a crucial role in determining their microstructure, which further influences their adsorption, swelling, release, and other functional properties.[6−8]

There are many reports on the preparation methods of cellulose-based microspheres in the literature. For instance, Zhang et al.[9] utilized the sol−gel phase conversion method to fabricate three-dimensional porous cellulose microspheres. However, achieving a uniform particle size proved challenging, and the process necessitated substantial quantities of organic solvents. Alternatively, Zhang et al.[10] employed a microfluidic approach to produce porous cellulose acetate microspheres, which required a specialized microfluidic device that was difficult to control and was incapable of generating millimeter-scale microspheres. In a different study, Wagh et al.[11] synthesized ketorolac methylamine-supported ethyl cellulose microspheres/nanospheres via the spray drying method, which facilitated the rapid production of large-scale microspheres with a narrow particle size distribution. Nonetheless, the unique drying process led to surface collapse of the microspheres, resulting in irregular morphologies, and the high-temperature conditions were not conducive to the incorporation of highly active substances. Additionally, Zhang et al.[12] achieved cellulose carboxylate microspheres through an emulsification-curing technique, but this method required numerous cross-linking agents and organic solvents, rendering the process complex and challenging to apply in the food industry.

The solubility and microstructure of CMC are different from those of cellulose. Generally, the formation of microspheres with application value needs cross-linking reactions and

Received: October 25, 2024
Revised: January 16, 2025
Accepted: January 17, 2025
Published: January 30, 2025

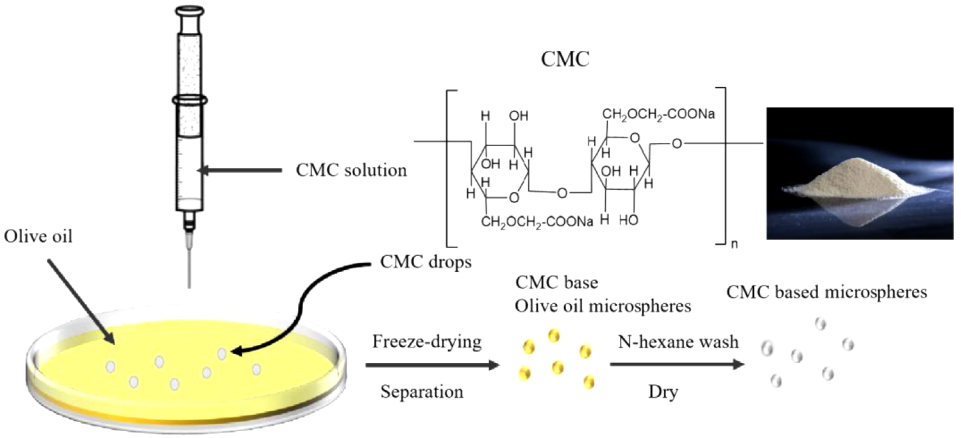

Figure 1. Schematic diagram of the preparation process of CMC-based microspheres by the dropping method.

material composites. The chemical cross-linking method is a typical technique for preparing CMC-based microspheres. In this process, CMC is initially dissolved in an aqueous phase, followed by the addition of cross-linking agents such as glutaraldehyde[13] and epichlorohydrin.[5,14] The CMC solidifies into spherical structures through various cross-linking reactions. In the ion cross-linking method, CMC drops are added to a salt solution containing Ag^{2+}[15] or Cu^{2+},[16] etc. The mixture is stirred to facilitate cross-linking, and the cross-linked microspheres are obtained after filtration. The use of the cross-linking method to prepare CMC microspheres takes several hours to cross-link, while using a variety of chemicals such as $AgNO_3$ (cross-link for 2 h) and $CuSO_4$ (cross-link for 4 h), not only consumes more time but also increases the preparation cost, and ion exchange occurs easily when Ag^+ or Cu^{2+} is present in the salt solution, which increases the difficulty of material reuse. The application of $AgNO_3$ or $CuSO_4$ solutions for cross-linking not only elevates the production costs but also introduces a significant likelihood of incorporating Ag^+ or Cu^{2+} into the material. Elevated concentrations of Ag^+ and Cu^{2+} pose potential risks to human health. Furthermore, at low pH levels, Cu^{2+} may experience electrostatic repulsion from the adsorbent, thereby diminishing the adsorption efficiency. Additionally, the propensities of Ag^+ and Cu^{2+} for ion exchange hinder the recyclability of the materials.

In conclusion, contemporary methodologies for the synthesis of CMC-based microspheres generally require specific cross-linking agents and intricate processes. These approaches are complex, which leads to changes in the CMC molecular structure and nonuniform microsphere morphology. In view of the fact that both cellulose[17] and starch[18] can be prepared by the dropping method, this article intends to prepare CMC-based microspheres using a simple dropping method (CMC microspheres can be prepared by heating for only 15 min, which saves a lot of time compared to the cross-linking method) and investigate the effects of CMC concentration, needle aperture, and other factors on the particle size of the microspheres. By conducting a series of experimental optimizations and structural characterizations, we established a comprehensive scientific understanding of the preparation of CMC-based microspheres via the dropping method. This approach seeks to achieve the preservation of the complete molecular structure and uniform morphology of CMC-based microspheres. Additionally, the application performance of these microspheres was validated by loading olive oil and vitamin C (VC), so as to promote the greater application of CMC-based microspheres in related fields.

2. MATERIALS AND METHODS

2.1. Materials. CMC (food grade, high viscosity, CAS: 9004-32-4) was purchased from Shanghai Changguang Enterprise Development, China. Gallino Extra Virgin Olive Oil (food grade, CAS: 8001-25-0) was purchased from Yiwu Guangpei Trading, China. *n*-Hexane, analytical reagent (AR, CAS: 110-54-3) was bought from Sinopharm Group Chemical Reagent, China. Cellulase (food grade, 50,000 U/g, CAS: 9012-54-8) was bought from Nanning Pangbo Bioengineering, China. Sodium chloride (AR, CAS: 7647-14-5) was purchased from Huizhou Zhicheng Chemical Technology, China. Corn starch (food grade, CAS: 9005-25-8) was bought from Guangzhou Shenchuang Chemical, China. α-Amylase (medium temperature, 20,000 U/g, CAS: 9000-90-2) was obtained from Qingdao Hyvison Biotechnology, China. VC (AR, CAS: 50-81-7) was obtained from Heilongjiang Xinhecheng Biotechnology, China.

2.2. Methods. *2.2.1. Preparation of CMC-Based Microspheres.* Appropriate optimization was carried out on the basis of the method of Zuo et al.[19] The effects of the concentration of CMC solution (3%, 5%, 7%, 9%, 11%) and needle aperture (22G needle, outer diameter 0.70 mm, inner diameter 0.41 mm; 24G needle, outer diameter 0.55 mm, inner diameter 0.29 mm; 26G needle, outer diameter 0.45 mm, inner diameter 0.23 mm; 27G needle, outer diameter 0.40 mm, inner diameter 0.21 mm) on the particle size of the microspheres were investigated. When the concentration of the CMC solution was investigated, the needle type was fixed at 27G. When the diameter of the needle was studied, the CMC concentration was controlled at 11%. The specific experimental methods were as follows.

Carboxymethyl cellulose (CMC) was configured into aqueous solutions of different concentrations (3%, 5%, 7%, 9%, 11%). The solutions were then heated at 80 °C and stirred for 15 min. Following this, the CMC solutions were aspirated by using a syringe. Olive oil, maintained at 25 °C, served as the dispersed phase. The CMC solution was uniformly dispensed into the dispersed phase from a height of approximately 15 cm using needles of various types, at a rate of approximately one drop per second (Figure 1). To minimize droplet adhesion, the syringe was translated during the dispensing process. The dispersed phase was then precooled at −50 °C for 3 h,

https://doi.org/10.1021/acsomega.4c09736
ACS Omega 2025, 10, 4754−4762

followed by vacuum freeze-drying and filtration to obtain solidified CMC-based olive oil microspheres.

Approximately 50 mg of CMC-based olive oil microspheres were subjected to ultrasonic cleaning in 20 mL of *n*-hexane for 10 min. After filtration, the microspheres were dried in an oven at 50 °C for 30 min. This procedure was repeated more than three times until the mass difference of the microspheres before and after cleaning was less than 0.05 mg to obtain CMC-based microspheres.

The drop process was investigated based on the particle size of CMC-based olive oil microspheres. The obtained CMC-based olive oil microspheres were placed in a microscope observation station with a standard line of 1 cm as the basis and a microscope magnification of 6 times. The particle size was measured by measuring the maximum diameter of the microsphere. The "average particle size ± standard deviation" of the CMC-based olive oil microspheres can be calculated by the arithmetic mean value and standard deviation of the particle sizes of each group of 5 microspheres.

2.2.2. Preparation of CMC-Based VC Microspheres. 2.0 g of CMC was dissolved in 16.0 g of distilled water and heated at 80 °C for 10 min. The CMC solution was cooled to 30 °C, then a certain amount of VC was added and dissolved completely, and the VC concentration (the ratio of VC mass to the total mass of VC and CMC) was set at 10%, 20%, 30%, 40%, and 50%, respectively. The mixed solution of CMC and VC was absorbed using a syringe and dropped into the dispersed phase at a constant speed through a 27G needle. The CMC-based VC microspheres were prepared according to the method in the previous section.

2.3. Characterizations. *2.3.1. Scanning Electron Microscopy (SEM) Morphology Analysis.* The samples were each mounted on the SEM sample stage using conductive adhesive. Specifically, the powder sample required uniform pressing followed by the removal of any unpressed powder via blowing. Subsequently, all sample surfaces were coated with a thin layer of gold. The SEM analysis was conducted at an acceleration voltage of 10 kV. Morphological observations and imaging of the samples were performed using a scanning electron microscope (S-4800, Hitachi, Tokyo, Japan).

2.3.2. Fourier-Transform Infrared (FT-IR) Spectroscopy Analysis. The samples were analyzed using FT-IR spectroscopy with an IR Spirit-T 100 instrument. A sample (1.0 mg) was placed into a mortar, combined with an appropriate amount of potassium bromide to achieve a sample-to-potassium bromide ratio of 1:100, and thoroughly ground before being pressed into a flake. The analysis was conducted at room temperature (20−25 °C) with a spectral resolution of 4 cm^{-1}, covering a measurement range of 4000−400 cm^{-1}. The scanning rate was set to 32 scans per minute, and each sample was tested in triplicate.

2.3.3. X-ray Diffraction (XRD) Analysis. The appropriate amount of sample was weighed and placed in the sample tray, and the sample was scanned by an X-ray diffractometer (D8 Advance, Bruker, Berlin, Germany) equipped with Cu-Kα radiation. Scanning conditions: the acceleration voltage was 40 kV, the current was 30 mA, the scanning rate was 10° min^{-1}, and the diffraction pattern was recorded in the 2θ range of 4−70°.

2.4. Loading and Release Property of CMC-Based Microspheres. *2.4.1. Loading Efficiency of CMC-Based Olive Oil Microspheres.* During the process of the dropping method, olive oil was used as the dispersed phase of the CMC-based microspheres. Full loading was achieved in the solidification and molding processes of the microspheres. The olive oil loading of the CMC-based olive oil microspheres can be directly calculated by measuring the mass of the CMC-based olive oil microspheres and the cleaned CMC-based microspheres through the same dropping method:

$$L = \frac{M_2 - M_1}{M_2} \times 100\% \quad (1)$$

L refers to the loading of olive oil, M_1 represents the mass of the CMC-based microsphere (g), and M_2 represents the mass of the CMC-based olive oil microsphere (g).

2.4.2. Loading and Encapsulation Efficiency of CMC-Based VC Microspheres. UV spectrophotometry was used to detect the VC content, and the determination method referred to the method of Li et al.[20] with some improvements.

Acetic acid−sodium acetate buffer was prepared as follows: 54.6 g of sodium acetate and 29 mL of acetic acid (1 mol/L) were mixed, and the volume was adjusted to 500 mL with a pH of 5.5; 7.305 g of NaCl was dissolved in distilled water to make a final volume of 250 mL, resulting in a 0.5 mol/L NaCl solution.

Standard curve determination: 0.05 g of VC was fixed to 50 mL with the configured sodium chloride solution, and the pH was adjusted to 4.5 as the standard solution. 0.1 mL of the standard solution was diluted with the sodium chloride solution to concentrations of 1, 2, 4, 8, 10, and 20 μg/mL, respectively. The absorbance at 243 nm was measured with the sodium chloride solution as the contrast, and the absorbance−concentration standard curve was obtained: $Y = 0.03637X + 0.00009$ (Y: absorbance, X: the concentration of VC (μg/mL), R^2=0.99998).

5 mg of various CMC-based VC microspheres, along with their corresponding CMC-based microspheres, were combined with 0.16 g of cellulase (food-grade, 50,000 U/g) and 5 mL of acetoacetic acid−sodium acetate buffer. The resulting mixture was placed in a water bath at 30 °C, protected from light and enzymatically hydrolyzed for 1 h, followed by centrifugation. Subsequently, 2 mL of the supernatant was diluted with 0.5 mol/L sodium chloride solution to a final volume of 50 mL. Compared with the enzymolysis products of blank CMC microspheres, the absorbance was determined by UV spectrophotometry. The drug loading and encapsulation efficiency of CMC-based VC microspheres were calculated by a standard curve.

$$L = \frac{cNV}{M_3} \times 100\% \quad (2)$$

L refers to the VC loading, c represents the actual mass concentration of VC in CMC and microsphere (mg/mL), N represents the dilution ratio of the measuring solution, V denotes the total volume of the solution, and M_3 denotes the mass of CMC-based VC microsphere (mg).

The ratio of the drug loading efficiency of a CMC-based VC microsphere to its corresponding set VC concentration is the encapsulation efficiency.

2.4.3. Preparation and Determination of Corn Starch-Based VC Microspheres. The corn starch-based VC microspheres were prepared according to the method of Zuo et al.[19] and were compared with the CMC-based VC microspheres. The concentration of corn starch was maintained at 10%. A specified quantity of VC and 3.0 g of corn starch were

https://doi.org/10.1021/acsomega.4c09736
ACS Omega 2025, 10, 4754−4762

dissolved and dispersed in 27.0 g of distilled water. The VC concentration, defined as the ratio of the mass of VC to the combined mass of VC and corn starch, was adjusted to 10%, 20%, 30%, 40%, and 50%, respectively. The resulting mixture was heated at the gelatinization temperature of corn starch (75−80 °C) for 2−3 min to ensure complete dissolution. Subsequently, the solution was drawn into a 27G needle to prepare corn starch-based VC microspheres via the dropping method.

5 mg of different corn starch-based VC microspheres and corresponding corn starch-based microspheres were respectively mixed with 0.16 g of α-amylase (medium temperature, 20,000 U/g) and 5 mL of acetoacetic acid sodium acetate buffer, and the mixture was enzymatically hydrolyzed in a water bath at 25 °C away from light for 1 h, then centrifuged. 2 mL of supernatant was fixed with 0.5 mol/L sodium chloride solution to 50 mL. With the enzymolysis products of blank corn starch-based microspheres as contrast, the absorbance was determined by ultraviolet spectrophotometry and calculated by standard curve. The calculation method of 2.4.2 was used to obtain the drug loading and encapsulation efficiency of corn starch-based VC microspheres.

2.4.4. Release Rate of CMC-Based VC Microspheres. 5 mg of CMC-based VC microspheres was immersed in 50 mL of anhydrous ethanol. The mixture was stirred at 1500 rpm at varying temperatures (30, 40, and 50 °C) for 7 h. The VC content in the ethanol was determined at different times (1, 3, 5, and 7 h). The release rate, defined as the ratio of the VC content in ethanol to the initial drug loading efficiency of the CMC-based VC microspheres, was then calculated. This data was utilized to evaluate the release properties of the CMC-based VC microspheres.

3. RESULTS AND DISCUSSION

3.1. Morphology of CMC-Based Microspheres. As shown in Figure 2, the microscopic image of CMC-based olive oil microspheres at 11% CMC concentration and 27G needle size can be seen from the figure that the external morphology of the microspheres was similar and the main shape of the microspheres was smooth and flat with a moderate average size.

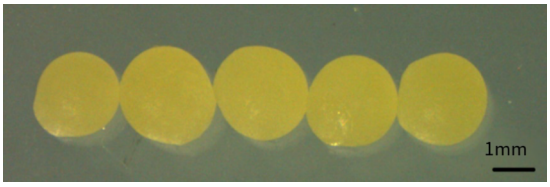

Figure 2. Micrograph of CMC-based olive oil microspheres.

The sizes of the five CMC-based olive oil microspheres were ascertained through microscopic analysis. The particle size was defined as the maximum diameter of the microspheres. The average particle size was obtained by calculating the mean value and standard deviation. As illustrated in Figure 2, the average particle size of the CMC-based olive oil microspheres was 1.955 ± 0.067 mm. Subsequent particle sizes were calculated by this method.

3.1.1. Influence of CMC Solution Concentration. Figure 3 illustrates that the particle size of CMC-based microspheres correspondingly decreased with the progressive increase in the concentration of the CMC solution. This phenomenon could be attributed to the concurrent increase in the solution's viscosity and the reduction in water content, which collectively lead to a more compact internal structure within the CMC microspheres. Consequently, the average particle size diminished, the standard deviation decreased, and the uniformity improved. The critical concentration for CMC microsphere formation was 11%. When the solution concentration exceeded 11%, the CMC solution no longer had fluidity and could not be prepared into microspheres by the dropping method. Therefore, 11% (critical concentration) was selected for the needle type test.

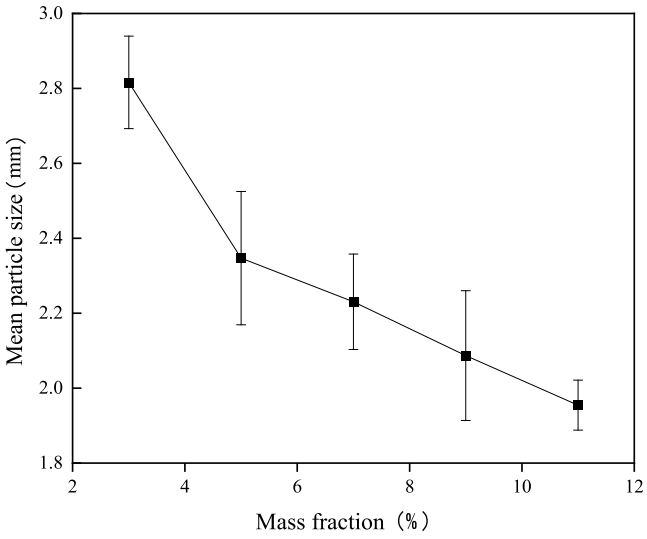

Figure 3. Effect of CMC mass fraction on the average particle size of CMC-based olive oil microspheres.

3.1.2. Effect of Needle Aperture. The effect of different needle apertures on the particle size of CMC-based olive oil microspheres was investigated with 11% solution concentration.

It can be seen from Table 1 that the average particle size of CMC-based olive oil microspheres and the standard deviation both increased with the increase of needle aperture, indicating that a 27G needle with a small aperture (inner diameter 0.21 mm) was more suitable for the preparation of uniform CMC-based olive oil microspheres.

The aperture of the needle not only changed the particle size of CMC-based olive oil microspheres but also affected the morphology of the microspheres. As shown in Figure 4, the 22G needle caused the microspheres to change from spheroid to ellipsoid; at the same time, the uniformity of the microspheres became worse. The evenness is determined by the size of the standard deviation. We have calculated the standard deviation of each group of samples in Table 1, and the standard deviation of 22G is the largest, so the evenness is the worst. At the same time, it can be seen from Figure 4 that compared with the roundness of CMC microspheres prepared by 27G needles, the microspheres prepared by 22G needles show a more irregular shape. The reason for this difference may be that as the size of the needle increases, the size of the droplet also increases, and the interaction between the droplet and the oil increases, so that the droplet cannot maintain a good shape.

Currently, the 27G needle represents the highest gauge compatible with the MULHE MH syringe available on the market. Consequently, needles with a gauge exceeding 27G

https://doi.org/10.1021/acsomega.4c09736
ACS Omega 2025, 10, 4754−4762

Table 1. Effect of Needle Aperture on Average Particle Size of CMC-Based Olive Oil Microspheres

	Average particle size of microspheres prepared with different needle apertures/mm			
	27G	26G	24G	22G
CMC-based olive oil microspheres	2.141 ± 0.071	2.641 ± 0.135	2.756 ± 0.156	3.114 ± 0.239

Figure 4. Microscope image of CMC-based olive oil microspheres with a needle size of 22G.

were not employed in this experiment. While the data did not reveal an inflection point, there was a notable trend of decreasing the average particle size and standard deviation of microspheres with larger needle sizes. Therefore, we concluded that the 27G needle provided the optimal conditions for this study.

By comprehensive comparison, the optimum preparation technology of CMC-based microspheres was determined as follows: the CMC concentration was 11%, and the needle size was 27G. Subsequent CMC-based microspheres, CMC-based olive oil microspheres, and CMC-based VC microspheres for structural characterization were prepared under these conditions.

3.2. Structural Characterization of CMC-Based Microspheres. *3.2.1. SEM Analysis.* Scanning electron microscopy analysis revealed that the raw CMC materials consisted of irregular fibrous particles with significant variations in particle size and morphology (Figure 5a). The surface of the CMC microspheres (Figure 5b,e,h) appeared slightly wrinkled, and the profile was a three-dimensional uniform polymer grid structure, closely resembling the state of CMC hydrogel microspheres post freeze-drying.[15] The CMC microspheres contained micropores ranging from 20 to 30 μm, primarily attributed to the sublimation of water molecules during the freeze-drying process.[5] This observation suggested a substantial adsorption capacity. The SEM images of CMC-based olive oil microspheres (Figure 5c,f,i) revealed that upon complete adsorption of olive oil, the surface smoothness of the microspheres was enhanced and the internal micropores were virtually eliminated. This indicated that CMC-based microspheres exhibit excellent adsorption properties for fat-soluble substances such as olive oil. The SEM images of CMC-based VC microspheres (solution concentration: 11%, needle aperture: 27G, VC concentration: 30%) (Figure 5d,g,j) revealed that after loading VC on the CMC microsphere, the surface of the microsphere retains folds, and the internal structure exhibited numerous micropores. However, the pore sizes were no longer uniform. This observation suggested that the water-soluble drug VC did not completely occupy the internal micropores of the CMC microspheres, potentially

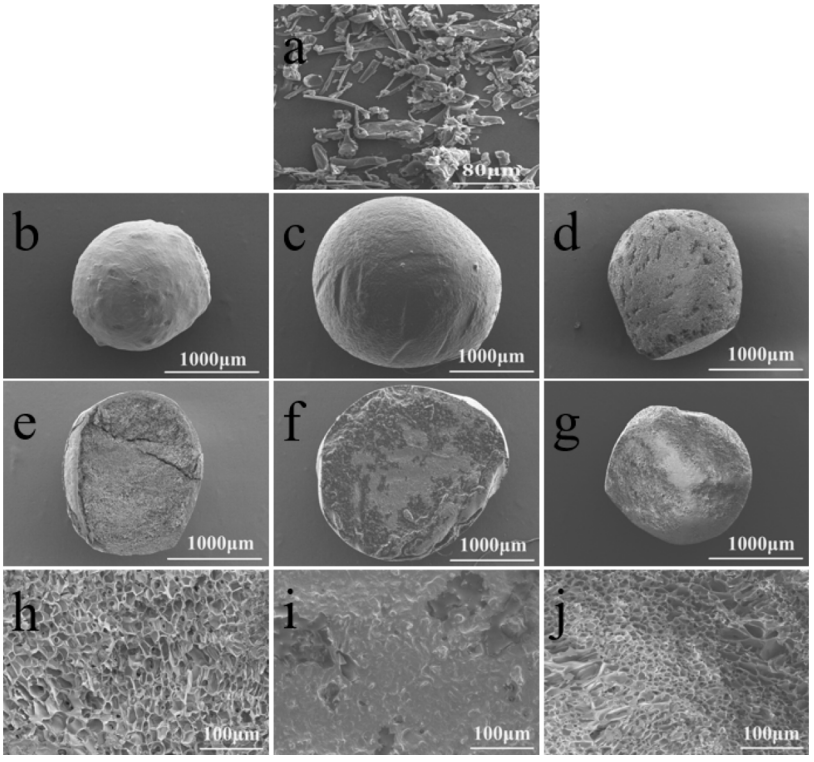

Figure 5. SEM images of CMC (a), CMC-based microsphere (b), CMC-based olive oil microspheres (c), CMC-based VC microspheres (d), corresponding section SEM images of CMC-based microsphere (e,h), corresponding section SEM images of CMC-based olive oil microspheres (f,i), and corresponding section SEM images of CMC-based VC microspheres (g,j).

https://doi.org/10.1021/acsomega.4c09736
ACS Omega 2025, 10, 4754−4762

leading to a lower drug loading efficiency compared to olive oil.

3.2.2. FT-IR Analysis. As illustrated in Figure 6, the FT-IR spectrum of CMC-based microspheres exhibited characteristic

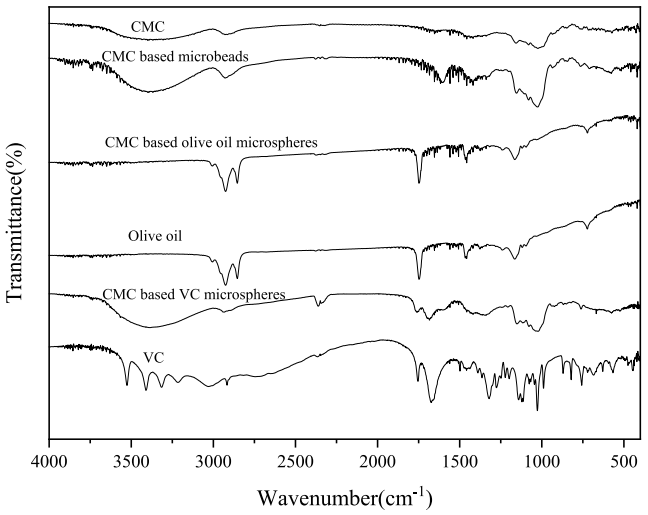

Figure 6. FT-IR spectra of CMC, olive oil, VC, CMC-based microspheres, CMC-based olive oil microspheres, and CMC-based VC microspheres (4000−400 cm^{-1}).

absorption peaks at 3319, 2921, and 1033 cm^{-1}, corresponding to the stretching vibrations of −OH, −CH, and C−O groups, respectively.[5] These peaks closely resembled the characteristic peaks, positions, and shapes observed in the FT-IR spectrum of CMC. This observation suggested that the functional groups of CMC-based microspheres remain largely unaltered during the preparation process, thereby confirming that the molecular structure of CMC was well preserved by this method. There were obvious differences between the FT-IR spectra of CMC-based olive oil microspheres and CMC-based microspheres. In the infrared spectra of CMC-based olive oil microspheres, the C−H stretching vibration peak of the saturated carbon chain was found at 2854 and 2925 cm^{-1}, the C═O stretching vibration peak was found at 1744 cm^{-1} and the methyl deformation vibration peak was found at 1461 cm^{-1}.[21] The characteristic peaks were attributed to olive oil. However, these peaks were absent in the CMC-based microsphere, suggesting the absence of residual olive oil within the CMC-based microsphere.[22] The characteristic peaks of CMC-based olive oil microspheres and pure olive oil display similar heights, locations, and shapes, which indicated a high drug loading efficiency of olive oil within the CMC-based microspheres. The characteristic peaks of VC were predominantly observed at 821, 1025, 1109, 1272, and 1754 cm^{-1}; among them, the peaks at 1754 and 1697 cm^{-1} caused by C═O double bond stretching vibration were reflected in the FT-IR spectra of CMC-based VC microspheres.

3.2.3. XRD Analysis. Figure 7 illustrated that CMC had an obvious diffraction peak at 2θ of 20.2° due to the semicrystalline nature of the CMC molecular chain.[23] Compared with CMC, multiple crystal diffraction peaks such as 16.1°, 22.1°, 28.3°, and 38.9° were added to CMC-based microspheres, and the diffraction peak at 20.2° basically disappeared. These results indicated that the crystallinity of CMC microspheres was significantly enhanced, and the formation of CMC-based microspheres changed the original

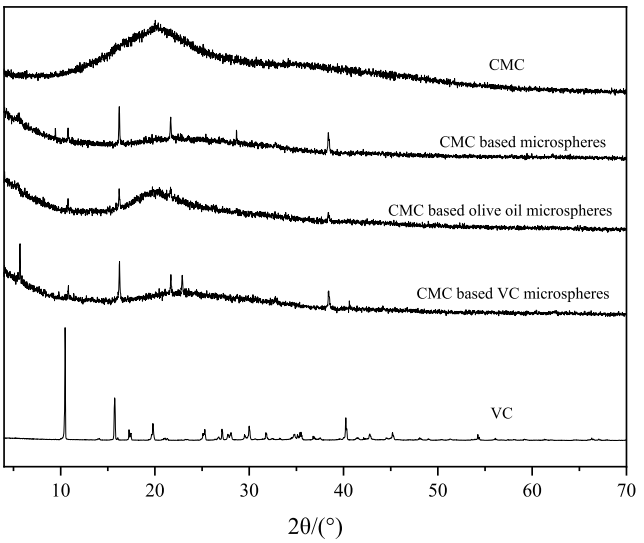

Figure 7. XRD patterns of CMC raw materials, CMC-based microspheres, CMC-based olive oil microspheres, and CMC-based VC microspheres and VC.

crystal structure of CMC.[24] Compared with CMC microspheres, the diffraction peaks of CMC olive oil microspheres at 2θ of 22.1°, 28.3°, and 38.9° basically disappeared, indicating that the crystal structure of CMC microspheres was covered by the loading of a large amount of olive oil. VC had a strong diffraction peak at 10.0°, but the diffraction peak moved to a lower angle and its intensity became weak after VC was loaded on the CMC microsphere. This indicated that VC was effectively wrapped by the CMC microsphere and its characteristic peak was weakened.[25]

3.3. Loading and Release Properties of CMC-Based Microspheres. *3.3.1. Loading Efficiency of CMC-Based Olive Oil Microspheres.* According to the method mentioned in Section 2.4.1, the drug loading efficiency of CMC-based olive oil microspheres was 82.18% ± 1.36%. This finding suggested that CMC-based microspheres exhibited excellent drug loading capacity for fat-soluble substances, and they could adsorb more than four times their own mass in olive oil. The superior drug loading efficiency could be attributed to the presence of numerous micropores within the CMC microspheres (Figure 5), facilitating strong direct adsorption and enhanced capacity for fat-soluble substances such as olive oil. The results were consistent with the data obtained from SEM and FT-IR. Currently, aside from the preparation of composite microcapsules loading fat-soluble substances via the complex coacervation method,[26] there are no documented instances of direct adsorption of low-melting-point fat-soluble substances by CMC microspheres. Moreover, the drug loading capacity of CMC microspheres is notably higher than that of other cellulose-based microspheres.

3.3.2. Loading and Release Properties of VC-Based Microspheres. 3.3.2.1. Loading and Encapsulation Efficiency of VC Microspheres. CMC concentration was set to 11%, and the needle aperture was set to 27G. The effects of the VC addition amount on the drug loading efficiency of different CMC-based VC microspheres and corn starch-based VC microspheres are shown in Figure 8.

As depicted in Figure 8, when the VC concentration increased from 10% to 30%, the drug loading and encapsulation efficiency of VC increased significantly. When

https://doi.org/10.1021/acsomega.4c09736
ACS Omega 2025, 10, 4754−4762

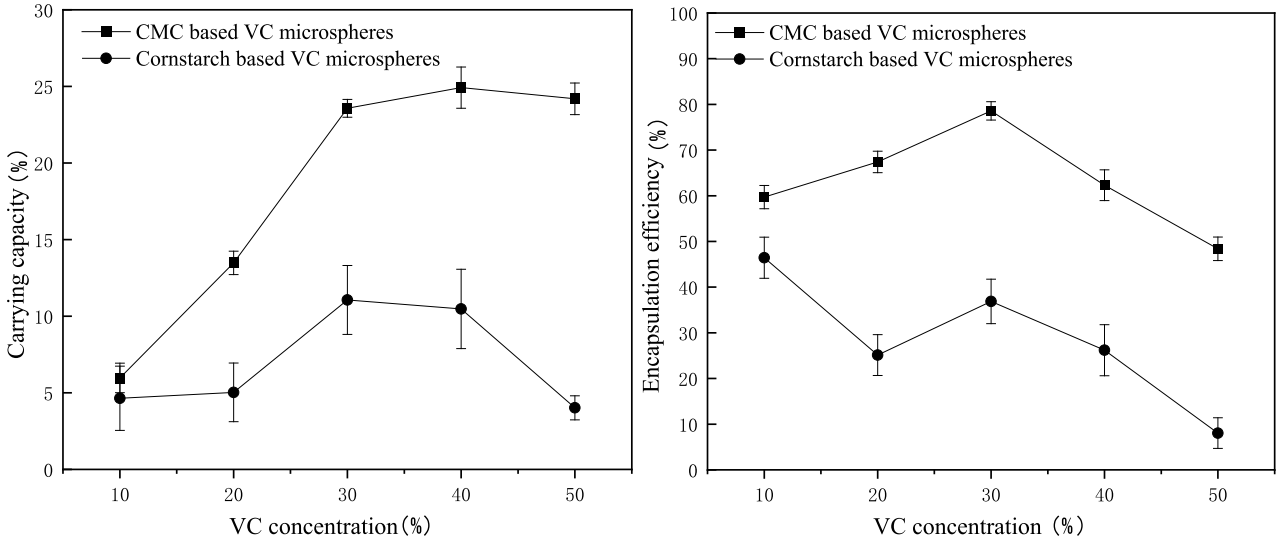

Figure 8. Effect of VC addition amount on drug loading and encapsulation efficiency of CMC-based microspheres and corn starch-based microspheres.

the VC concentration was 30%, 40%, and 50%, the VC drug loading efficiency of CMC-based VC microspheres was 23.57%, 24.92%, and 24.19%. These data indicated that the limit drug loading efficiency of VC was approximately 24%, with the maximum encapsulation efficiency (78.57%) being achieved at a VC concentration of 30%. Figure 5j demonstrates that numerous micropores remained in the CMC-based VC microspheres at a VC concentration of 30%. However, the drug loading efficiency was not enhanced through increasing the VC concentration, suggesting that the loading mechanism of CMC-based microspheres for water-soluble drugs with high melting points differs from their adsorption mechanism, and CMC microspheres on water-soluble drugs with high melting points were different from that of low melting point fat-soluble substances.

CMC-based VC microspheres were dissolved by cooling the CMC solution to 30 °C and then adding VC, while corn starch and VC were dissolved at the gelatinization temperature of corn starch (75−80 °C). Cooling could lead to the precipitation of corn starch, while high-temperature dissolution may also cause the rapid degradation of VC.[28] As shown in Figure 8, the drug loading efficiency of corn starch-based VC microspheres was significantly lower than that of CMC-based VC microspheres under the same VC concentration, which was mainly caused by the differences in the dissolution temperature and drug loading efficiency. However, the maximum drug loading efficiency of corn starch-based VC microspheres was achieved at 11.06% when the VC concentration was 30%. Beyond this concentration, the drug loading efficiency decreased, suggesting that the drug loading of VC in high concentration solutions decreased significantly at the gelatinization temperature of corn starch. Therefore, a 30% VC concentration remains the optimal addition amount.

Through comparative analysis, it had been determined that CMC-based microspheres exhibited superior film-forming properties than those of corn starch-based microspheres,[27] and their preparation conditions were milder, resulting in higher drug loading capacity and encapsulation efficiency of CMC-based VC microspheres based on sodium carboxymethyl cellulose,[27] leading to higher drug loading efficiency and encapsulation efficiency. This study further evaluated the release property of CMC-based VC microspheres prepared with a VC concentration of 30%.

3.3.2.2. Release Property of CMC-Based VC Microspheres in Ethanol. CMC was insoluble in ethanol, whereas VC exhibited slight solubility in ethanol. Consequently, this study evaluated the release properties of CMC-based VC microspheres in ethanol at various temperatures. Figure 9 illustrates

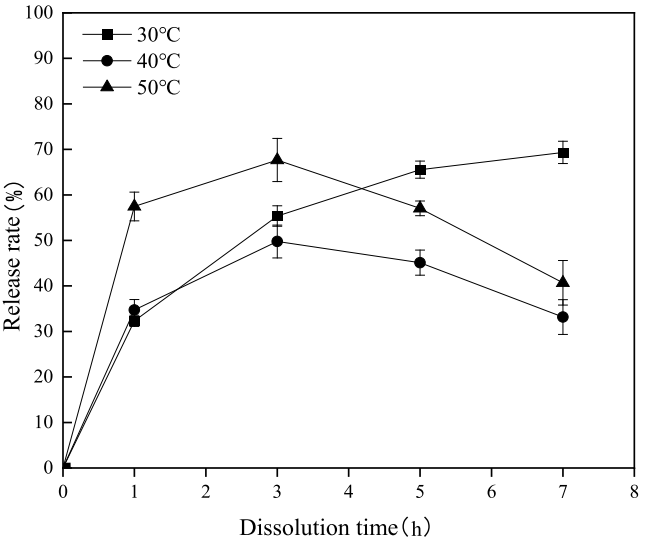

Figure 9. Effects of different temperatures and times on the release rate of CMC-based VC microspheres in ethanol.

that the release rate of VC in ethanol at 30 °C increased with the dissolution time, reaching 69.34% after 7 h. After dissolution for 1 h, the highest release rate of VC was observed at 50 °C in ethanol, followed by 40 °C, with the lowest release rate occurring at 30 °C. After 2 h, the release rate in ethanol at 40 °C decreased compared to that at 30 °C. After 5 h, the release rate in ethanol at 30 °C became the highest among the tested conditions. These findings indicated that VC undergoes substantial degradation in ethanol at both 40 and 50 °C, resulting in a more rapid release but more pronounced degradation at elevated temperatures.[29] The data

https://doi.org/10.1021/acsomega.4c09736
ACS Omega 2025, 10, 4754−4762

depicted in Figure 9 indicated that CMC-based VC microspheres could achieve sustained and stable release in ethanol at 30 °C. Nonetheless, an increase in temperature results in substantial degradation of VC.

4. CONCLUSIONS

In this study, CMC-based microspheres were prepared by using the dropping method. Compared with contemporary methods, the preparation method of CMC microspheres in this paper uses less time and cost. This straightforward technique not only preserves the complete molecular structure of CMC but also achieves the objectives of uniform morphology in the CMC-based microspheres and effective encapsulation of both fat- and water-soluble substances. The particle size of the CMC-based microspheres decreased with an increasing CMC solution concentration and decreasing needle aperture. The optimal preparation conditions were determined to be a CMC solution concentration of 11% and the use of a 27G needle. Under these conditions, the morphology of CMC olive oil microspheres exhibited a uniform morphology, minimum standard deviation of particle size, and an internal three-dimensional uniform polymer grid structure. The functional groups of the CMC-based microspheres did not change during the preparation process. However, multiple crystal diffraction peaks emerged, and the original characteristic peaks of CMC were predominantly absent, indicating a significant alteration in the original crystal structure of CMC. The drug loading efficiency of CMC-based microspheres for olive oil, which was a low melting point fat-soluble substance, achieved 82.18%. Conversely, the ultimate drug loading efficiency and maximum encapsulation efficiency for the water-soluble high melting point drug VC was approximately 24% and 78.57%, respectively. Furthermore, a sustained and stable release was observed in ethanol at 30 °C.

This study fabricated CMC-based microspheres exhibiting a uniform morphology and superior drug loading efficiency using a straightforward dropping method. The cross-linking method involves a relatively intricate preparation process, necessitating the use of cross-linking agents to facilitate the cross-linking reaction, thereby increasing both the complexity and the duration of preparation. In contrast, the preparation method proposed in this study is more straightforward and expedited. In this study, CMC microspheres with uniform morphology and high loading capacity were successfully synthesized by using a straightforward direct drip technique. The absence of organic solvents and other chemicals in the preparation process endows the microspheres with exceptional biocompatibility, making them suitable for direct application in the food and pharmaceutical industries. The CMC-based microspheres are synthesized without chemical reactions such as cross-linking, thereby preserving the complete molecular structure of CMC while incorporating functional substances. This confers them with excellent water solubility and in vivo digestibility, rendering them highly valuable as slow-release materials. Furthermore, the preparation method described herein is simple and cost-effective, does not require high-temperature treatment, and allows for repeated synthesis under standard laboratory conditions, highlighting its significant industrial applicability. These findings offer valuable insights for the functionalization of microspheres derived from cellulose and other natural polymer materials, promoting the application of cellulose- and CMC-based microspheres in related fields.

AUTHOR INFORMATION

Corresponding Authors

Tao Yuan − *School of Biological and Chemical Engineering, NingboTech University, Ningbo, Zhejiang 315100, China;* orcid.org/0009-0004-9354-6850; Email: 2648130687@qq.com

Dan Qiu − *School of Materials and Chemical Engineering, Ningbo University of Technology, Ningbo, Zhejiang 315211, China; School of Biological and Chemical Engineering, NingboTech University, Ningbo, Zhejiang 315100, China;* Email: qiudan_zju@163.com

Authors

Ling Wang − *School of Chemical Engineering, Ningbo Polytechnic, Ningbo, Zhejiang 315800, China*

De-Shuang You − *School of Chemical Engineering, Ningbo Polytechnic, Ningbo, Zhejiang 315800, China; School of Materials and Chemical Engineering, Ningbo University of Technology, Ningbo, Zhejiang 315211, China*

Dan-yan Guo − *School of Chemical Engineering, Ningbo Polytechnic, Ningbo, Zhejiang 315800, China; School of Materials and Chemical Engineering, Ningbo University of Technology, Ningbo, Zhejiang 315211, China*

Xue-Chen Zhuang − *School of Materials and Chemical Engineering, Ningbo University of Technology, Ningbo, Zhejiang 315211, China; Zhejiang Institute of Tianjin University, Ningbo, Zhejiang 315201, China*

Complete contact information is available at: https://pubs.acs.org/10.1021/acsomega.4c09736

Author Contributions

L.W.: investigation (lead); methodology (equal); writing—original draft (lead). D.-S.Y., X.-C.Z., and D.-y.G.: writing—review and editing (lead). D.Q. and T.Y.: project administration (lead); supervision (lead); writing—review and editing (equal). The photos in figures were taken by D.-S.Y. and D.-y.G.

Notes

The authors declare no competing financial interest.

ACKNOWLEDGMENTS

We thankfully acknowledge Zhejiang Province's Special Support Program (2023R5232) for the execution of this work.

REFERENCES

(1) Tu, H.; Zhu, M.; Duan, B.; Zhang, L. Recent progress in high-Strength and robust regenerated cellulose materials. *Adv. Mater.* **2021**, *33* (28), No. e2000682.

(2) Qiao, L.; Li, S.; Li, Y.; Liu, Y.; Du, K. Fabrication of superporous cellulose beads via enhanced inner cross-linked linkages for high efficient adsorption of heavy metal ions. *J. Cleaner Prod.* **2020**, *253*, 120017.

(3) Gericke, M.; Trygg, J.; Fardim, P. Functional cellulose beads: preparation, characterization, and applications. *Chem. Rev.* **2013**, *113*, 4812−4836.

(4) Gelaw, B. B.; Kasaew, E.; Belayneh, A.; Tesfaw, D.; Tesfaye, T. Review of the sources, synthesis, and applications of nanocellulose materials. *Polym. Bull.* **2023**, *81*, 7733−7735.

(5) Hu, J.; Huang, Y.; Yao, Y.; Pan, G.; Sun, J.; Zeng, X.; Sun, R.; Xu, J. B.; Song, B.; Wong, C. P. Polymer composite with improved thermal conductivity by constructing a hierarchically ordered three-dimensional interconnected network of BN. *ACS Appl. Mater. Interfaces* **2017**, *9*, 13544−13553.

https://doi.org/10.1021/acsomega.4c09736
ACS Omega 2025, 10, 4754−4762

(6) Xu, W.; Gao, X.; Tan, H.; Li, S.; Zhou, T.; Li, J.; Chen, Y. Covalent and biodegradable chitosan-cellulose hydrogel dressing containing microspheres for drug delivery and wound healing. *Mater. Today Commun.* **2022**, *33*, 104163.
(7) Zong, Y.; Zhang, Y.; Lin, X.; Ye, D.; Luo, X.; Wang, J. Preparation of a novel microsphere adsorbent of prussian blue capsulated in carboxymethyl cellulose sodium for Cs(I) removal from contaminated water. *J. Radioanal. Nucl. Chem.* **2017**, *311*, 1577−1591.
(8) Kong, Q.; Wang, X.; Lou, T. Preparation of millimeter-sized chitosan/carboxymethyl cellulose hollow capsule and its dye adsorption properties. *Carbohydr. Polym.* **2020**, *244*, 116481.
(9) Zhang, D.-Y.; Wan, Y.; Yao, X.-H.; Chen, C.; Ju, Y.-X.; Shuang, F.-F.; Fu, Y.-J.; Chen, T.; Zhao, W.-G.; Liu, L.; Li, L. Fabrication of three-dimensional porous cellulose microsphere bioreactor for biotransformation of polydatin to resveratrol from *Polygonum cuspidatum* Siebold & Zucc. *Ind. Crops Prod.* **2020**, *144*, 112029.
(10) Zhang, M.; Guo, W.; Ren, M.; Ren, X. Fabrication of porous cellulose microspheres with controllable structures by microfluidic and flash freezing method. *Mater. Lett.* **2020**, *262*, 127193.
(11) Wagh, P.; Mujumdar, A.; Naik, J. B. Preparation and characterization of ketorolac tromethamine -loaded ethyl cellulose micro-/nanospheres using different techniques. *Part. Sci. Technol.* **2019**, *37* (3), 347−357.
(12) Zhang, H.; Luan, Q.; Li, Y.; Wang, J.; Bao, Y.; Tang, H.; Huang, F. Fabrication of highly porous, functional cellulose-based microspheres for potential enzyme carriers. *Int. J. Biol. Macromol.* **2022**, *199*, 61−68.
(13) Tan, Z.; Zhang, L.; Zhang, Q. Preparation and properties of polyvinyl alcohol/sodium carboxymethyl cellulose crosslinking microspheres. *China Plast. Ind.* **2015**, *43*, 41−44.
(14) Chang, C.; Duan, B.; Cai, J.; Zhang, L. Superabsorbent hydrogels based on cellulose for smart swelling and controllable delivery. *Eur. Polym. J.* **2010**, *46*, 92−100.
(15) Guo, J.; Yao, H.; Li, X.; Chang, L.; Wang, Z.; Zhu, W.; Su, Y.; Qin, L.; Xu, J. Advanced hydrogel systems for mandibular reconstruction. *Bioact. Mater.* **2023**, *21*, 175−193.
(16) Maslamani, N.; Khan, S. B.; Danish, E. Y.; Bakhsh, E. M.; Akhtar, K.; Asiri, A. M. Metal nanoparticles supported chitosan coated carboxymethyl cellulose beads as a catalyst for the selective removal of 4-nitrophenol. *Chemosphere* **2022**, *291*, 133010.
(17) Kamthai, S.; Magaraphan, R. Mechanical and barrier properties of spray dried carboxymethyl cellulose (CMC) film from bleached bagasse pulp. *Ind. Crops Prod.* **2017**, *109*, 753−761.
(18) Weng, L.; Le, H. C.; Talaie, R.; Golzarian, J. Bioresorbable hydrogel microspheres for transcatheter embolization: preparation and in vitro evaluation. *J. Vasc. Interventional Radiol.* **2011**, *22*, 1464−1470.
(19) Zuo, R.; Qiu, D.; Yang, Q. Preparation and characterization of starch-based microspheres by dropping method. *Fine Chem.* **2024**, 1−14.
(20) Li, Y.; Dong, X.; Yao, L.; Wang, Y.; Wang, L.; Jiang, Z.; Qiu, D. Preparation and characterization of nanocomposite hydrogels based on Sself-assembling collagen and cellulose nanocrystals. *Polymers* **2023**, *15*, 1308.
(21) Pan, J.; Liao, G.; Su, R.; Chen, S.; Wang, Z.; Chen, L.; Chen, L.; Wang, X.; Guo, Y. ^{13}C Solid-state NMR analysis of the chemical structure in petroleum coke during idealized in situ combustion conditions. *ACS Omega* **2021**, *6*, 15479−15485.
(22) Wang, N.; Ga, L.; Ai, J.; Wang, Y. Fluorescent copper nanomaterials for sensing NO_2^- and temperature. *Front. Chem.* **2022**, *9*, 805205.
(23) Zhang, W.; Liu, K.; Wang, T.; Liu, Y.; He, W.; Pei, J.; Yang, J.; Duan, H.; Yu, X.; Qin, G.; Chen, Q. Tough and self-healing all-in-one supercapacitor enabled by triple-network redox carrageenan and sodium carboxymethyl cellulose reinforcing gel polymer electrolyte. *J. Alloys Compd.* **2024**, *1006*, 176106.
(24) Ma, H.; Zhao, Y.; Lu, Z.; Xing, R.; Yao, X.; Jin, Z.; Wang, Y.; Yu, F. Citral-loaded chitosan/carboxymethyl cellulose copolymer hydrogel microspheres with improved antimicrobial effects for plant protection. *Int. J. Biol. Macromol.* **2020**, *164*, 986−993.
(25) Desai, K. G.; Liu, C.; Park, H. J. Characteristics of vitamin C immobilized particles and sodium alginate beads containing immobilized particles. *J. Microencapsulation* **2005**, *22*, 363−376.
(26) Tan, R.; Shen, J.; Dong, W.; Zhang, Z.; Long, Y.; Hu, R.; Chen, Z.; Jiang, K. Preparation of green coffee oil microcapsules by complex coacervation method and its physicochemical properties. *Food Sci.* **2020**, *41*, 144−152.
(27) Zhang, P.; Ai, Z.; Li, M. Research of the characteristic of edible cornstarch film. *Packag. Eng.* **2005**, *26*, 59−61.
(28) Fan, C.; Yin, Y.; Zhang, P. Critical control points and stability study of VC detection in food for special medical purposes. *Food Industry* **2023**, *44*, 142−147.
(29) Yin, X.; Chen, K.; Cheng, H.; Chen, X.; Feng, S.; Song, Y.; Liang, L. Chemical stability of ascorbic acid integrated into commercial products: a review on bioactivity and delivery technology. *Antioxidants* **2022**, *11*, 153.

https://doi.org/10.1021/acsomega.4c09736
ACS Omega 2025, 10, 4754−4762